Forest Systems
27 (3), e019, 12 pages (2018)
eISSN: 2171-9845
https://doi.org/10.5424/fs/2018273-13857
Instituto Nacional de Investigación y Tecnología Agraria y Alimentaria O. A., M. P. (INIA)

RESEARCH ARTICLE

OPEN ACCESS

National assessment of throughfall sensitivity to changes in storm magnitude for the forests of Iran

Pedram Attarod[1,2], Qiuhong Tang[2], John T. Van Stan II[3] and Xingcai Liu[2]

[1]Forestry and Forest Economics Department, Faculty of Natural Resources, University of Tehran, Iran. [2]Key Laboratory of Water Cycle and Related Land Surface Processes, Institute of Geographic Sciences and Natural Resources Research, Chinese Academy of Sciences, China. [3]Department of Geology and Geography, Georgia Southern University, USA.

Abstract

Aim of study: To understand throughfall (TF) sensitivity to variability in rainfall amount (P_g) for typical forest sites across the main climate types of Iran.

Area of study: Nine forest stands of several common native and introduced tree species situated in all common Iranian climate types, but located primarily in northern Iran.

Material and methods: A nondimensional relative sensitivity coefficient was employed to predict responses of TF to P_g changes. Projected P_g changes over the measurement sites for the period 2020-50 were estimated using one of the Coupled Model Intercomparison Project phase 5 (CMIP5) known as HadGEM2-ES under low and high emission scenarios (RCP 2.6 and 8.5).

Main results: TF displayed strong positive linear relationships with P_g at all sites [$TF=0.66\ P_g\ -0.16$; $R^2=0.91$]. The sensitivity coefficient ranged from 0.96-2.35 across the nine forest sites and large sensitivity coefficient differences were found between small (< mean annual P_g) and large (> mean annual P_g) storms for arid and Mediterranean plantations. Shifts in P_g and increased small storm frequency are predicted for these regions (2020-50) under low and high emission scenarios.

Research highlights: TF sensitivity may be a useful variable when selecting tree species for afforestation to buffer expected shifts in P_g due to climate change.

Additional keywords: climate change; forest ecosystems; precipitation projection; throughfall sensitivity.

Authors´ contributions: Pedram Attarod: Design and conception; Qiuhong Tang: Financial support; John T. Van Stan II: Language editor and scientific comments, and Xingcai Liu: Data preparation.

Citation: Attarod, P., Tang, Q., Van Stan II, J-T., Liu, X. (2018). National assessment of throughfall sensitivity to changes in storm magnitude for the forests of Iran. Forest Systems, Volume 27, Issue 3, e019. https://doi.org/10.5424/fs/2018273-13857

Received: 27 Aug 2018. **Accepted:** 03 Dec 2018.

Funding: This research was supported by the University of Tehran (UT), Iran and by the International Partnership Program of Chinese Academy of Sciences (Grant No. 131A11KYSB20170113) and the National Natural Science Foundation of China (Grant No. 41790424).

Competing interests: The authors have declared that no competing interests exist.

Correspondence should be addressed to Pedram Attarod: attarod@ut.ac.ir

Introduction

A significant portion of rainfall is intercepted on forest canopy surfaces, where it is either returned to the atmosphere as interception or redistributed to the ground as throughfall (TF) and stemflow. This rainfall partitioning by forest cover significantly alters hydrologic cycling along the soil-forest-atmosphere continuum (Miralles *et al.*, 2010) and can impact feedbacks between the hydrologic cycle and global climate (Davies-Barnard *et al.*, 2014). Stemflow is the proportion of rainfall that drains to the ground along the stem, usually accounting for <2% of annual rainfall in most forests (Van Stan & Gordon, 2018). The remaining majority (60-90%) of rainfall passes through canopy gaps or drips from the vegetation, reaching the surface as TF (Levia *et al.*, 2011) where it can influence soil moisture (Raat *et al.*, 2002), physicochemistry (Rosier *et al.*, 2015), fine root distribution (Ford & Deans, 1978), and microbial processes (Moore *et al.*, 2016). As these ecohydrological interactions play key roles in ecosystem functioning, understanding TF's response to natural and anthropogenic variability is critical to forest management.

Studies across forest ecosystems agree that rainfall amount (P_g) is the principal variable driving stand-scale TF amount (Levia & Frost 2006; Levia *et al.*, 2011)—often explaining >90% of inter-storm TF variability—and that TF-P_g relationships are shaped by canopy structures, like leaf area index, crown

depth, etc. (Staelens *et al.*, 2008; Toba & Ohta 2005). However, the authors are unaware of previous work quantifying TF sensitivity to changes in P_g—a commonly anticipated climate response to hydrologic intensification (Huntington, 2006). This is surprising since hydrologic intensification has been linked to increased extreme P_g in many regions (*c.f.*, Tollefson, 2016). Moreover, afforestation, reforestation, urban forestry and other "greening" initiatives have grown in popularity and, therefore, increased the forest cover in most developed regions (*i.e.*, McGovern & Pasher, 2016). In Iran, for example, the restoration of semi-arid and arid ecosystems through planting of low-demand and drought tolerant species has become a critical element of national ecosystem management plans (Attarod *et al.*, 2015b).

Iran has invested in vast tree-plantings throughout its major cities for urban greening and air pollution mitigation, including the Chitgar and Lavizan Forest Parks (Sadeghi *et al.*, 2016) and the ongoing "Jam Afforestation Project" which is tasked with large-scale afforestation and reforestation in the Zagros region (FRWO, 2012). Restoration of the natural Caspian deciduous forests (that extend from the Alborz Mountains to the southern coast of the Caspian Sea) has also resulted in significant reforestation projects since the 1960s (Abbasian *et al.*, 2015). Concerns have risen over the impact of these greening initiatives on the hydrological cycle (Sun *et al.*, 2006; Wang *et al.*, 2011), particularly for the 90% of Iran classified as arid or semi-arid (Ul Hassan *et al.*, 2007). The first process in the rainfall-to-runoff pathway is the partitioning of P_g by forest canopies (Savenije, 2004) and, accordingly, an improved understanding of TF sensitivity to climate change and P_g is essential for addressing these concerns and quantifying the impacts of Iran's (and other nations') large-scale afforestation and reforestation efforts.

A sensitivity analysis is a technique used to determine how different values of an independent variable impact a particular dependent variable under a given set of assumptions. A method for estimating the "sensitivity coefficient" of a dependent variable (in this case, TF) on the relative changes of an independent variable (in this case, P_g) exists (McCuen, 1974) and has been rigorously applied to evapotranspiration and its principal meteorological drivers (Hupet & Vanclooster, 2001). However, the authors are unaware of its application to assess sensitivity of TF to its principal meteorological driver, P_g, for multiple species of contrasting canopy structure. Thus, the objectives of this study are to (1) collect rainfall and TF across common forest species of differing canopy structures and climates in Iran, then (2) quantify and compare their TF sensitivity coefficients. Accomplishing these aims will provide novel information to complement existing data used by forest managers during species selection for restoration and afforestation activities.

Materials and Methods

Sites description

Data were collected in 9 forest stands of several common native and introduced tree species (Table 1) situated in all common Iranian climate types (Table 2), but located primarily in northern Iran (Fig. 1). The selected species represent a diversity of forest canopy architectures, ranging from the smooth-barked, broad-leaved canopy of *Fagus orientalis* (FO) to the rough-barked, needle-leaved canopy of *Pinus eldarica* (PE). Leaf phenology also differs among the selected species as, for example FO is deciduous and PE is evergreen. The PE and *Cupressus arizonica* (CA) throughfall sites are in southern Alborz Mountain Range near the city of Tehran, while the remaining sites—FO, *Quercus castaneifolia* (QC_1-QC_3), *Acer velutinum* (AV), *Pinus brutia* (PB), *Cupressus sempervirens* var. *horizontalis* (CS)—are in northern Alborz Mountain Range and Southern coasts of the Caspian Sea (Fig. 1). Stand structural (and TF) measurements for each forest stand were performed in 0.5 ha plots. Stand density ranged from 112 trees ha^{-1} in the FO forest to 1,600 trees ha^{-1} in the CS plantation (Table 1). Diameter at breast height (1.3 m, dbh) varied greatly among the measured forests, with the smallest values in CS (12 cm) and the largest values in QC_3 (65 cm) (Table 1). Mean canopy coverage also exhibited a wide range across sites, from 45% for CS and 95% for FO (Table 1).

Meteorological data were obtained from the nearest synoptic meteorological stations recording reliable long-term meteorological data (Fig. 1). The range in meteorological data records is from 1951 to 2015 (Table 2). There exists relatively long distances between the Mehr-Abad, Sari, and Gorgan meteorological stations (Fig. 1), but there is no significant topography between the measurement sites and the meteorological stations, and no closer meteorological stations exist in the region. Due to lack of meteorological station inside the Caspian forest, we used meteorological data recorded by Nou-Shahr meteorological station regardless of elevation difference. The ranges of annual precipitation (P) and temperature (T) in the weather station sites are 16.4-17.4 ºC and 230-1291 mm, respectively (Table 2). The ''De Martonne'' climate classification, *i.e.*, De Martonne aridity index (I_{DM}), as described by Baltas (2007), ranged roughly from 49 to 8.5, so that the study sites

Table 1. Forest sites where throughfall (TF) data were collected, including their climate, geographical coordinates, elevation, and stand characteristics. "G" and "D" refer to growing and dormant seasons, respectively, and dbh refers to diameter at breast height.

Species	Code	Climate^	Elevation (m)	Longitude	Latitude	Mean dbh (cm)	Mean height (m)	Closure (%)	Density (trees ha^{-1})	Study period (year)	Storms (n)
Fagus orientalis	*FO*	VH	1410	51º37'	36º35'	50	32	95	112	08, 09 (G)	53
Quercus castaneifolia	QC_1	VH	1550	51º37'	36º35'	36	28	80	175	09, 10 (G)	28
Quercus castaneifolia	QC_2	SH	360	52º14'	36º28'	21	18	70	864	12 (G)	20
Acer velutinum	*AV*	SH	360	52º14'	36º28'	20	19	80	292	12 (G)	20
*Pinus brutia**	*PB*	SH	360	52º14'	36º28'	14	12	85	541	12 (G)	20
Quercus castaneifolia	QC_3	M	250	55º14'	37º15'	65	21	55	198	13 (G)	24
Cupressus sempervirens var. *horizontalis*	*CS*	M	250	55º14'	37º15'	12	7	70	1600	13 (G)	24
*Pinus eldarica**	*PE*	A	1220	51º08'	35º42'	22	9	60	1020	11-14 (G, D)	165
*Cupressus arizonica**	CA	A	1220	51º08'	35º42'	20	8	45	960	11-14 (G, D)	165

*Non-native. ^VH: Very humid, SH: Semi-humid, M: Mediterranean, A: Arid. See text for climate classification method.

Table 2. Details of weather stations included in this study, their climate types according to the De Martonne aridity index (I_{DM}: Baltas, 2007), and the duration of their measurement record.

Station	Dates of record	Elevation (m asl)	Longitude	Latitude	Annual temperature (ºC)	Annual precipitation (mm)	Climate (I_{DM} value)
Nou-Shahr	1977-2015	-21	51º30'	36º39'	16.4	1291	Very humid (49)
					16.4	1291	Very humid (49)
Sari	1985-2015	23	53º00'	36º33'	16.9	742	Semi-humid (27)
					16.9	742	Semi-humid (27)
					16.9	742	Semi-humid (27)
Gorgan	1955-2015	0	54º24'	36º54'	17.8	572	Mediterranean (21)
					17.8	572	Mediterranean (21)
Mehr-Abad	1951-2015	1191	51º19'	35º41'	17.4	230	Arid (8.5)
					17.4	230	Arid (8.5)

were grouped into very humid (FO, QC_1), semi-humid (QC_2, AV, PB), Mediterranean (QC_3, CS), and arid (PE, CA) climates (Table 1).

Field measurements

Field measurements were performed from July-2008 to March-2014 during growing and dormant seasons (Table 1). A discrete rain event was defined as a period with >0.1 mm of rainfall. The minimum inter-event dry period between discrete storms was 4-10 h, depending on the site. The effect of pre-storm canopy wetness was assumed negligible as the canopy is assumed to be dry after the minimum inter-event time, which is a common assumption among rainfall partitioning studies (Carlyle-Moses & Gash, 2011). Snowfall was ignored. P_g at each forest site was measured by 3-10 funnel-type plastic collectors with 10 cm funnel diameter and 20-30 cm heights, placed in the nearest open area away from the forest stands. The average of water amount measured in all rain-gauges at a site was used to estimate P_g for each site. Quantities of water in the collectors were measured manually using a graduated cylinder. Storms that reached only the weather stations but not the forest sites, or vice versa, were ignored. P_g volumes were measured at the same time as TF volumes at each site,

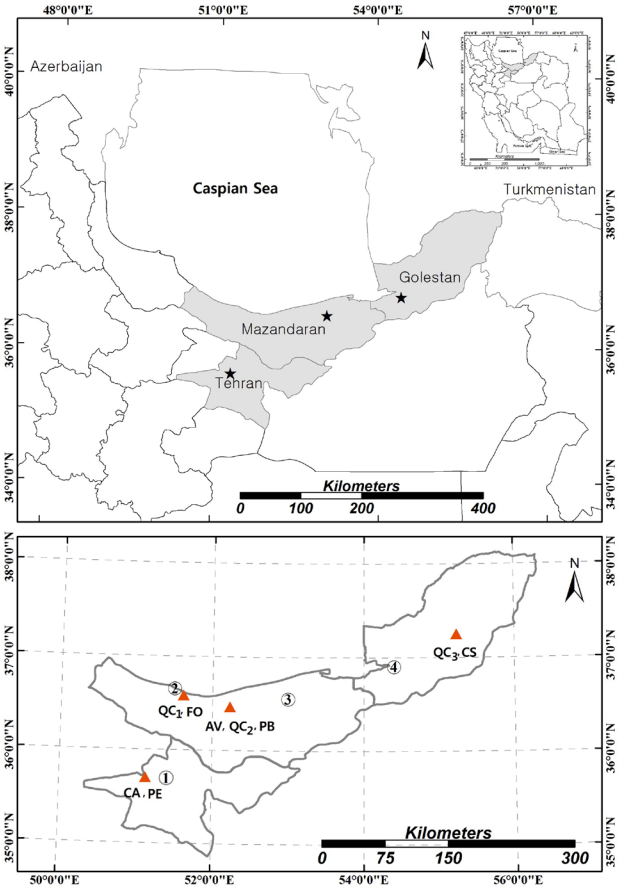

Figure 1. Locations of the measurement sites (triangles) and synoptic meteorological stations (numbers) in the northern provinces of Iran. See Tables 1 and 2 for species abbreviations. Meteorological stations are numbered as: (1) Mehr-Abad; (2) Nou-Shahr; (3) Sari; and (4) Gorgan.

either immediately after a storm or at sunrise following a night storm.

TF was measured using 20-50 rain collectors of the same design as those used to quantify P_g. TF collectors were randomly distributed beneath the canopy and fabric covered the neck of the collectors to avoid litter, needles, and debris from entering (Abbasian *et al.*, 2015). TF data based on multiple field campaigns that used a different number of collectors is a common, often necessary, issue in national-to-international scale studies (*i.e.*, Wallace *et al.*, 2013; Návar, 2017); however, it is important to note that this methodological variability may introduce uncertainty to the stand-scale TF estimates (Vose *et al.*, 2016). Variability about mean P_g and TF will be expressed in standard error (SE) throughout.

Throughfall sensitivity coefficients

A practical method of presenting a sensitivity analysis is to plot relative changes of a dependent variable (in this case, TF) against relative change of an independent variable (*i.e.*, P_g) as a curve (*e.g.*, Singh & Xu, 1997; Goyal, 2004, Attarod *et al.*, 2015a). This is different from a standard regression of TF versus P_g (Fig. 2a) as the mean sensitivity coefficient is calculated as the slope of a correlation between the percent changes in P_g against percent changes in TF (Fig. 2b). The sensitivity coefficient represents the fraction of change in P_g transmitted to the change of TF, *i.e.* a sensitivity value of 0.1 would suggest that a 10% increase in P_g may be predictable to increase TF by 1%. Negative coefficients would indicate that a decrease in TF would result from an increase of P_g, which is not expected due to the universally reported positive relationship between P_g and TF (Friesen *et al.*, 2015). In the present study, the sensitivity coefficient of TF was determined in climate classifications only in response to changes in P_g on an event-basis.

Projected P_g changes over the measurement sites

General Circulation Models (GCMs) are numerical models representing physical processes in the atmosphere, ocean, cryosphere, and land surface. These models are the most advanced tools currently available for simulating the response of the global climate system to increasing greenhouse gas concentrations. GCM simulations for the fifth Assessment Report (AR5) of the Intergovernmental Panel on Climate Change (IPCC) have become available (Taylor *et al.*, 2012; Miao *et al.*, 2014). Comparing to the IPCC AR4, the GCMs in AR5 include a more varied set of model types (*i.e.*, climate/earth system models with more interactive components such as atmospheric chemistry, aerosols, dynamic vegetation, ice sheets and carbon cycle) (Liu *et al.*, 2013). Several improvements in the physics, numerical algorithms and configurations are implemented in the IPCC AR5 models with a new set of scenarios called Representative Concentration Pathways (RCPs) for energy and industry CO_2 emissions (Moss *et al.*, 2010). The RCPs span a large range of stabilization, mitigation and non-mitigation pathways. Phase 5 of the Coupled Model Intercomparison Project (CMIP5) is a standard experimental protocol for studying the output of GCMs which provides a community-based infrastructure in support of climate model diagnosis, validation, intercomparison, documentation and data access (Jones *et al.*, 2011). Longer time-scale ("centennial") experiments have been performed at the Met Office Hadley Centre with the HadGEM2-ES Earth System model—one of the CMIP5 climate models (Collins *et al.*, 2011; Jones *et al.*, 2011; Miao *et al.*, 2014). The HadGEM2-ES model used here is one of the state-of-the-art GCMs and involves many typical and advanced

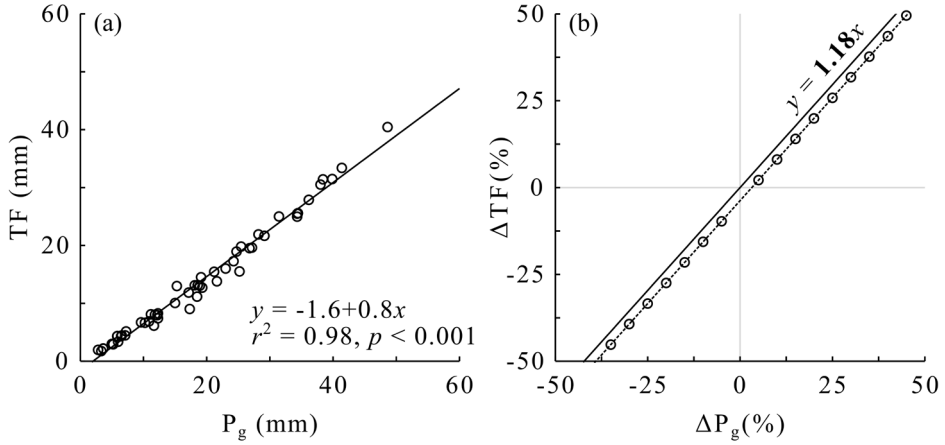

Figure 2. Example regression of throughfall (TF) against storm magnitude (P_g) for data collected at the *Fagus orientalis* site. Through shifting P_g by any percentage (ΔP_g), the regression equation (in panel a) can be used to calculate a corresponding percent change in TF (ΔTF). These shifts are (b) plotted and a regression calculated where the slope is a nondimensional coefficient of "sensitivity."

representations of land and ocean processes (Jones *et al.*, 2011). The HadGEM2-ES climate data has been widely used for climate studies (Huntingford *et al.*, 2013). The *r1i1p1* ensemble of HadGEM2-ES was used in this study. The *r1i1p1* ensemble is the most accessible ensemble in the CMIP5 archive.

To understand P_g variations under changing climate over the measurement sites, we focused on the precipitation projection for two scenarios: RCP 2.6 and RCP 8.5. RCP 2.6 represents a "low" emissions scenario featured by the radiative forcings of 2.6 Wm^{-2} and atmospheric CO_2 concentration of 421 ppm by 2100. RCP 8.5 represents a "high" emission scenario with the radiation forcing of 8.5 Wm^{-2} and CO_2 concentration of 936 ppm by 2100. The time resolution of projected storm magnitude (*i.e.*, P_g) is daily. Future climate data in grids with 0.5°×0.5° horizontal resolution across measurement sites were obtained from the HadGEM2-ES model projections (Hempel *et al.*, 2013).

Delta change method

Because of the limitations of coarse-resolution GCM climate data (used in these predictions), the delta change (DC) method is generally used to derive scenarios of future climate (*e.g.*, Fischer *et al.*, 2007; Shahid, 2011; Chung & Nkomozepi, 2012). The method consists of simply scaling the observed climate data using monthly change factors calculated from the differences in climatology predicted by GCMs for the current and future periods. In this way, P_g for future time periods was derived by scaling the historically observed climate data (OBS) by the GCM-computed change. This results in a new P_g time series scaled according to the GCMs, but based on historical observations. In this study, the OBS from 1974 to 2004 (reference period) were scaled to derive the 30-yr future climate scenario for the period 2020-2050. Relative change factors (ΔVar) were then applied to the observed flux variable to calculate future P_g. Following Leng & Tang (2014), the DC method are formulated as Eq., (1):

$$\begin{aligned} &\mathrm{Var}_{\Delta}(i,j) = [\mathrm{Var}_{\mathrm{OBS}}(i,j)][\Delta\mathrm{Var}(j)]; \\ &i = 1,2,\ldots\ldots 31; \quad j = 1,2,\ldots\ldots 12, \end{aligned} \tag{1}$$

where Var_{Δ} is the scaled flux variable using the DC method and $\mathrm{Var}_{\mathrm{OBS}}$ is the observed flux variable in the historic period. The suffixes i and j stand for the day and the month, respectively, and ΔVar is the monthly DC factor, which is calculated as follows:

$$\Delta\mathrm{Var}(j) = \frac{\overline{\mathrm{Var}}_{\mathrm{future}}(j)}{\overline{\mathrm{Var}}_{\mathrm{current}}(j)}; \qquad j = 1,2,\ldots\ldots,12 \tag{2}$$

where $\overline{\mathrm{Var}}_{\mathrm{future}}$ (j) and $\overline{\mathrm{Var}}_{\mathrm{current}}$ (j) are the mean values of the time series for month j for the future and current time periods by GCMs.

Results

Overview of rainfall and throughfall events

There were 290 P_g events recorded from 2008-2014 across all measurement sites and P_g ranged from 0.5-54.7 mm. Mean P_g was 10.8±0.7 mm across all forest sites, but site-specific mean P_g ranged from 17-20 mm for forests in the very humid, semi-humid, and Mediterranean climate types (Table 3). Mean P_g from the arid forest sites was 4.4 mm (Table 3). At arid sites,

Table 3. Characteristics of recorded rainfall events (P_g) in the measurement sites with respect to the different climate types. n refers to the number of recorded events.

Climate type	n	Mean (mm)	Max (mm)	Min (mm)	SE (mm)	%< Mean	%< 5 mm	%>15 mm
Very Humid	81	20.0	50.9	2.8	1.4	58	13	85
Semi-humid	20	17.3	35.0	0.5	2.4	45	25	65
Mediterranean	24	19.4	54.7	0.5	3.0	58	29	62
Arid	165	4.4	19.0	0.5	0.3	67	70	5

67% of collected storms were < mean P_g; however, for other climate types, this fraction was generally around 50% (Table 3). "Large" storms (P_g > 15 mm) were frequent at the very humid forest sites (85%), yet only 5% of storms exceeded 15 mm at arid sites (Table 3). "Small" storms (P_g < 5 mm) were the norm for arid forests in this study (70%: Table 3). The respective percentages of P_g < 5 mm or P_g > 15 mm were similar for the semi-humid and Mediterranean forests (Table 3).

Strong positive linear relationships between event mean TF and P_g were observed across all sites [TF=0.66 (P_g) - 0.16; R^2 = 0.91] and at each individual site (Table 4). Slopes of the regression lines between TF and P_g (often assumed to be linked to varying canopy structures) were wide-ranging: 0.39 for CS to 0.81 for FO (Table 4). Relative TF (TF:P_g) varied roughly from 40% (Mediterranean CS) to 75% (very humid QC_1) (Table 4). In arid and Mediterranean climates, minimum TF:P_g were measured at zero, however, in other climates the minimum was approximately 47% (Table 4). TF:P_g was, surprisingly, nearly the same when averaged for all the needle-leaved forests (55.2%) and broad-leaved forests (50%) across the climate zones (Table 4). Marked differences in TF:P_g on average, however, were observed for plantations versus natural forests, where plantations were found to produce 53.4% of TF compared to 71.9% for natural forests. For all sites, QC_1 produced the highest TF:P_g in very humid conditions (QC_1: 74.5%) and the lowest TF:P_g under Mediterranean conditions (CS: 39.3%) (Table 4). Generally higher standard errors were observed for TF:P_g in the Mediterranean (3.25%) and arid sites (3.35%) compared to forests in other climates (1.34%) (Table 4).

Historical annual storm characteristics

Historical records at the meteorological stations show that mean annual precipitation decreased from very humid (1291 mm y^{-1}) to arid climate (230 mm y^{-1}) (Table 5). Compared with other climates, the arid climate had relatively constant annual precipitation, varying only by 9 mm y^{-1} between 1951-2015 (Table 5). The ratio of maximum P_g to mean annual precipitation was respectively 11%, 16%, 18%, and 22% for the semi-humid, very humid, Mediterranean, and arid climates (Table 5). Although mean P_g had a descending trend from very humid (10.5 mm) to arid (3.9 mm), the proportion of mean P_g to maximum P_g in different climates ranged from 8.5% in the semi humid climate to 5.0% in the very humid climate (Table 5).

Throughfall sensitivity to changes in storm magnitude

TF exhibited varying degrees of sensitivity to P_g, showing large fluctuations (*i.e.*, doubling in sensitivity)

Table 4. Relationships between throughfall (TF) and rain event magnitude (P_g), percent of event based average relative throughfall (TF: P_g), and related statistics. See Table 1 for the tree species represented by the location codes. n refers to the number of recorded events.

Tree species	n	Mean TF: P_g (%)	Max TF: P_g (%)	Min TF: P_g (%)	SE TF: P_g (%)	Regression	r^2
FO	53	69.4	85.0	52.1	1.3	TF=0.81 P_g -1.60	0.98
QC_1	28	74.5	87.8	60.1	1.1	TF=0.80 P_g -0.92	0.99
QC_2	20	66.4	80.0	45.4	1.3	TF=0.70 P_g -0.17	0.97
AV	20	44.2	59.2	30.9	1.3	TF=0.54 P_g -1.03	0.96
PB	20	59.0	78.6	43.7	1.7	TF=0.62 P_g -0.55	0.91
QC_3	24	58.4	88.3	0	3.1	TF=0.57 P_g -0.88	0.87
CS	24	39.3	76.0	0	3.4	TF=0.39 P_g -0.64	0.80
PE	165	50.7	86.8	0	3.9	TF=0.79 P_g -0.50	0.98
CA	165	55.8	89.2	6.0	2.8	TF=0.73 P_g -0.34	0.97

Table 5. Historical characteristics of annual precipitation, number of storms, and other related rain event magnitude (P_g) characteristics recorded in the meteorological stations nearest to the measurement sites.

Station Climate (Record)	Annual precipitation (mm)			P_g (mm)	
	Mean ± SE	Max.	Min.	Mean	Max.
Nou-Shahr Very humid (1977-2015)	1291±30	1628	921	10.5	208
Sari* Semi-humid (1985-2015)	742±28	1007	442	7.2	85
Gorgan Mediterranean (1955-2015)	577±17	962	314	6.0	105
Mehr-Abad Arid (1951-2015)	230±9	403	100	3.9	50

*event number is for the period 2000-2015 (1666 events); In the very humid, Mediterranean, and arid climates, 4819, 5762, and 3772 events were recorded, respectively.

for species planted in different climates (Fig. 3). TF from the arid PE forest was most sensitive to fluctuations in P_g (= 2.35) and TF from the Mediterranean QC_3 forest was least sensitive (= 0.96) (Fig. 3). Needle-leaved plantations (*i.e.*, PE, CA) generally had higher sensitivity (> 1.5) to changing P_g compared to broadleaved forests (~ 1.0) (Fig. 3). For broadleaved forests, QC_1 was less sensitive than FO in a very humid climate (Fig. 3). QC_1, QC_2, and QC_3 had similar sensitivity coefficients regardless of climate: very humid (=1.09) to semi-humid (=1.07) and Mediterranean climates (= 0.96) (Fig. 3). TF sensitivity was tested for larger and smaller storm sizes than the mean P_g in each climate (Table 6). Excluding AV, PB, and QC_1, TF was found to be more sensitive to small storms (Table 6). Plantations in arid or Mediterranean climates had large differences in sensitivity coefficient between small and large events, *e.g.* 2.95 *vs.* 1.14 for PE and 1.78 *vs.* 0.74 for CS plantation (Table 6). Interestingly, the FO forest had nearly identical sensitivity values for storms smaller (1.06) and larger (1.05) than mean P_g (Table 6). Sensitivity of the very humid QC_1 natural forest was greater for large events (1.07 against 1.24) in comparison with the semi-humid QC_2 and Mediterranean QC_3 forests (Table 6).

Projected changes in annual precipitation and storm magnitude

During the 2020-2050 period, the low emissions (RCP 2.6) scenario predicted increased annual precipitation on average in all climate types, excluding the semi-humid climate, yet the high emissions (RCP 8.5) scenario predicted decreased annual precipitation on average in all climates excluding the arid climate (Table 7). Projected changes to mean P_g from the low emission scenario was +16.0%, +3.2%, 0%, and -1.8% for Mediterranean, very humid, arid, and semi-humid forests, respectively (Tables 5 and 7). The high emissions scenario predicts that mean P_g will change by -5% in very humid forests and -10% in arid forests, but mean P_g will not change for forests in the Mediterranean and semi-humid climates (Tables 5 and 7).

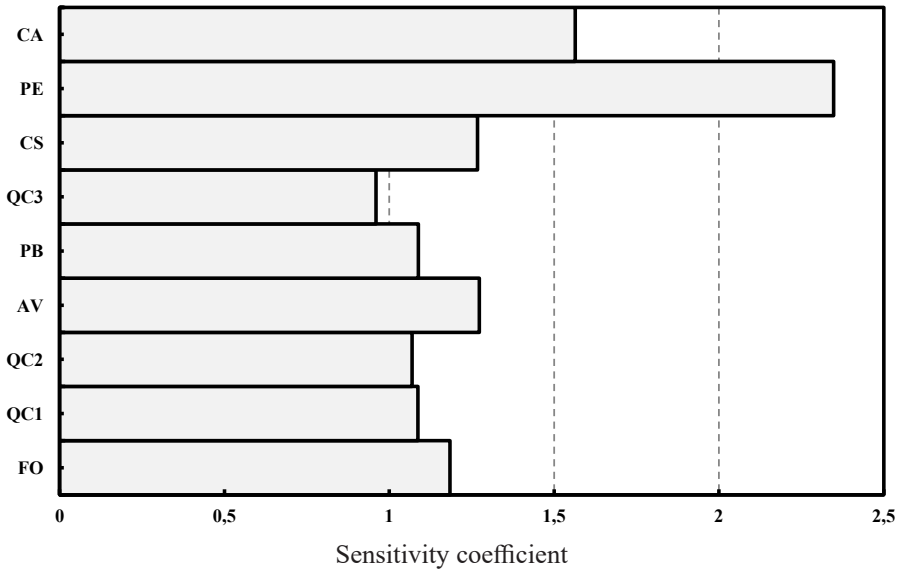

Figure 3. Mean throughfall (TF) sensitivity coefficients for the measurement sites. See Table 1 for the tree species represented by the location codes.

Table 6. Throughfall (TF) sensitivity coefficients classified for storm magnitudes (P_g) smaller and larger than mean P_g recorded in the measurement sites. See Table 1 for the tree species represented by the location codes.

Tree species	Mean P_g (mm)	Mean sensitivity for < mean P_g	Mean sensitivity for > mean P_g
FO	18.9	1.06	1.05
QC_1	23.2	1.07	1.24
QC_2	17.3	1.08	0.81
AV	17.3	1.14	1.34
PB	17.3	0.96	1.45
QC_3	19.4	1.20	0.80
CS	19.4	1.78	0.74
PE	4.4	2.95	1.14
CA	4.4	1.57	1.21

Table 7. Projections of annual precipitation, and mean storm magnitude (P_g) during the period of 2020-2050 predicted by the GCM under RCP 2.6 (low emission), and RCP 8.5 (high emission) scenarios.

Climate	Annual precipitation (mm)			P_g (mm)
	Mean±SE	Max.	Min.	Mean
Very humid				
RCP 2.6	1306±34	1587	871	10.8
RCP 8.5	1207±31	1489	845	10.0
Semi-humid				
RCP 2.6	736±28	989	563	7.0
RCP 8.5	670±24	903	515	7.2
Mediterranean				
RCP 2.6	598±18	867	405	7.0
RCP 8.5	518±16	743	357	6.0
Arid				
RCP 2.6	271±13	448	144	3.9
RCP 8.5	247±11	391	139	3.5

Discussion

Storm magnitude and throughfall

We collected a wide range of storms across sites hosting common forests in all of Iran's climate types (Tables 1-2; Fig. 1). Stands for which comparable TF data exist (*e.g.*, FO and QC_1) are comparable to those reported elsewhere, for example: FO versus *Fagus sylvatica* (*e.g.*, Staelens *et al.*, 2008) and QC versus *Quercus serrata* and *Quercus acutissima* (*e.g.*, Toba & Ohta, 2005). Relationships between P_g and TF for individual forest often indicate differences in the canopy-meteorological interactions that control TF production by plants (Zhang *et at.*, 2016). In this study, as in others, P_g accounted for most (nearly all) of TF variability regardless the species, yet the slope and intercept of the P_g-TF correlation varied across the forests of differing species-climate combination (Table 4). Relative TF:P_g in our study, 39.3-74.5%, appears to be strongly tied to forest structure (*e.g.*, density, seasonal change, vegetation area index, gap fraction, and canopy storage capacity), and climate conditions (P_g and, perhaps storm intensity and wind conditions) as shown by many others (Crockford & Richardson, 2000; 2011; Staelens *et al.*, 2008; Muzylo *et al.*, 2012; Motahari *et al.*, 2013). Results indicated that, when the same species experiences different climate conditions, they can differentially partition P_g into TF—something particularly evident QC in three different climates (Table 4).

Throughfall sensitivity to storm amount

Large fluctuations in TF sensitivity were observed between different species, climate types, and storm sizes (greater or less than mean annual P_g) common to Iran (Table 6). For forest managers, it is apparent that different species selected for planting in different climates will exhibit differing TF sensitivities to shifting P_g (Fig. 3). Practically, managers can use these sensitivity coefficients (Fig. 3 or Table 6) and projected changes to P_g (Tables 5 versus 7) and estimate the potential shift in TF supply to the forest surface. For example, PE's sensitivity coefficient (2.35) indicates that a 10% decrease in P_g could approximately reduce TF by 23%. Although we identified little change in the total yearly precipitation in the arid climate for the most recent decade (where these PE plantations are generally situated), an approximate estimation of 8% decrease in the storm size observed in the recent decade can induce an 18% decrease in TF in these plantations. Greater sensitivity coefficients for PE (and CA) plantations may be a result of (1) these species having larger storage capacities than other tree species in this study (Sadeghi *et al.*, 2015), (2) their arid climate allowing their canopies to dry more efficiently between storms, and (3) most-to-nearly all the storms being small (Table 6). The higher sensitivity of these species to P_g has implications for forest managers dealing with climate change, since both are the most widely-used species for afforestation in the arid and semiarid regions of Asia (*e.g.*, Iran, Lebanon, Syria, Pakistan, Iraq, and Afghanistan) and are frequently selected due to their greater tolerance to drought, high/low temperature extremes, and being faster-growing than native broad- or needle-leaved tree species (Jazirei, 2009). Under a changing climate, water resource management in arid regions is therefore complicated by afforestation initiatives and forest managers may be able to use TF sensitivity as a variable in their decision to choose a

species with the least sensitivity to expected shifts in P_g.

The remaining species located in the Caspian forests of northern Iran with very humid, semi-humid and Mediterranean climates exhibited roughly the same sensitivity (mean = 1.13; Fig. 3). However, according to our results, the replacement of QC_3 natural forest with CS man-made in the Mediterranean areas of the eastern Caspian region will likely increase TF sensitivity by 0.31 (Fig. 3). This increased TF sensitivity with converting Mediterranean QC forests to CS may be a product of greater tree density of young CS (Table 1) or, more theoretically, greater roughness lengths and zero-plane displacement heights (Rutter *et al.*, 1975; Valente *et al.*, 1997). Moreover, CS's scale-like needle-leaves have different leaf shedding habits compared to QC_3's broadleaves, which will differentially interact with P_g to alter TF and its sensitivity (Pypker *et al.*, 2011).

Natural broad-leaved forests in the Caspian region (FO and QC_1) showed roughly the same sensitivity (Fig. 3). The primary function of the Caspian forests, other than wood production, is conservation of soil and water resources (Sagheb Talebi *et al.*, 2014). Thus, it is expected that the low TF sensitivity of FO and QC_1 to shifts in P_g will help buffer the region against climate changes. But, restoration of the Caspian deciduous forest of northern Iran by planting species, like CS (which had a greater TF sensitivity coefficient), were extensively performed by Iran's Forest, Rangeland, and Watershed organization, and may have considerable effects on ecosystem ecohydrology through altered TF supply. In contrast, introduction of PB in the semi humid climate of the central Caspian region for restoration of degraded forests showed roughly the same, even lower, sensitivity compared to native species (AV and QC_2) (Fig. 3). Thus, understanding the relationship between hydrologic cycling and the impact of afforestation projects on these variables can be useful for forest management and selection of suitable species for reforestation of degraded forest ecosystems.

Although the consistently-observed strong correlation between stand-scale TF and storm amount across forest types and climates confirms that storm amount is the primary factor affecting TF generation after canopy structures are saturated (Levia *et al.*, 2011), the degree to which stand-scale TF responds to storm amount has been linked to vegetation structure (leaf area index, crown depth, etc.) (Staelens *et al.*, 2008; Toba & Ohta 2005). Consequently, it is advisable to incorporate vegetation characteristics with TF sensitivity in response to changes in P_g responses in future investigations.

Combining throughfall sensitivity and climate projections

Changes in P_g to an area are expected to be compounded by the TF sensitivity of each forest type. An example "rough" estimation using the 16% increase in P_g predicted by RCP 2.6 scenario in the Mediterranean climate results in a 20% and 15% increase in TF generation in CS and QC_3 forests, respectively. The projected 3.2% increase (by RCP 2.6) and 5% decrease (by RCP 8.5) in mean P_g, however, in the very humid climate of Iran where the Caspian forests are located (Table 7) is not anticipated to significantly alter TF supply to the forest floor due to the tree species' low sensitivity (Fig. 3). Despite the highest sensitivity of plantations in the arid climate (~2), very slight changes in mean P_g are predicted by the RCP 2.6 scenario which may not influence TF receipt at the surface. However, under the RCP 8.5 scenario, a 10% decrease in mean P_g in the arid climate could decrease TF by 23% and 15% per event beneath PE and CA plantations, respectively. Fewer impacts may be realized in the semi-humid climate where the dominant tree species showed low TF sensitivity and not significant changes in mean event size are predicted by both RCPs. Clearly, these climate change scenarios (and others) can be a reference for setting minimum and maximum configurations of forest cover in water management and planning associated with adaptation. There will be large uncertainty among GCM models, most GCM models may have different performances across regions, and, as a consequence of lacking large scale observations, downscaling from GCM grid data to local areas is difficult. Moreover, the delta change factor strategy used in this study does not adjust climate projections, but assumes that the signal or changes are reasonably projected by climate models, even though the models are biased (Leng & Tang, 2014). A key feature of this approach is that, because the method uses historical precipitation as its basis and GCM data only to change the magnitude of the historical precipitation, it fails to account for changes in P variability predicted by different GCM models (Leng & Tang, 2014). Still, the projections and downscaling of changes in P_g under the most conservative (low emission) and the highest greenhouse gas emissions pathway (high emission) scenarios (Table 7) underscores the necessity of work to understand TF sensitivity of common forest types in a region.

Conclusion

This national assessment of throughfall beneath common forest types in Iran showed large fluctuations

in throughfall sensitivity for species planted in different climates. Arid needle-leaved plantations exhibited generally higher sensitivity responses to changing storm amount, while very humid, natural broad-leaved forests had low sensitivity responses. Projections of mean storm magnitude under a low emission scenario indicated that, compared to historical data, modest changes would be expected for most climates (excluding arid) on average during 2020-2050. However, under a high emission scenario, larger alterations are expected in all climate types except the arid climate. Results indicate that any projected change in storm size will not simply be translated directly to a change in throughfall. Rather, the increase or decrease in throughfall amount may be better predicted as a product of the projected change in storm magnitude and the forest-specific throughfall sensitivity. These findings have implications for selection of the most appropriate and adapted species for afforestation under climate change.

References

Abbasian P, Attarod P, Sadeghi SMM, Van Stan II JT, Hodjati SM, 2015. Throughfall nutrients in a degraded indigenous Fagus orientalis forest and a Picea abies plantation in North of Iran. Forest Syst 24(3) e035. https://doi.org/10.5424/fs/2015243-06764

Attarod P, Kheirkhah F, Khalighi Sigaroodi Sh, Sadeghi SMM, 2015a. Sensitivity of reference evapotranspiration to global warming in the Caspian region, North of Iran. J Agr Sci Tech-Iran 17: 869-883.

Attarod P, Sadeghi SMM, Pypker TG, Bagheri H, Bagheri M, Bayramzadeh V, 2015b. Needle-leaved trees impacts on rainfall interception and canopy storage capacity in an arid environment. New Forest 46: 339-355. https://doi.org/10.1007/s11056-014-9464-2

Baltas E, 2007. Spatial distribution of climate indices in northern Greece. Meteorol Appl 14: 69–78. https://doi.org/10.1002/met.7

Carlyle-Moses DE, Gash JHC, 2011. Precipitation interception loss by forest canopies. In: Levia DF, Carlyle-Moses D, Tanaka T (eds) Forest hydrology and biogeochemistry: synthesis of past research and future directions. Ecolog studies 216: 407–424.

Chung SO, Nkomozepi T, 2012. Uncertainty of paddy irrigation requirement estimated from climate change projections in the Geumho River basin, Korea. Paddy Water Environ 10: 175–185. https://doi.org/10.1007/s10333-011-0305-z

Collins WJ, Bellouin N, Doutriaux-Boucher M, Gedney N, Halloran P, Hinton T, Hughes J, Jones CD, Joshi M, Liddicoat S, *et al.*, 2011. Development and evaluation of an Earth-system model HadGEM2. Geosci Model Dev 4: 997–1062. https://doi.org/10.5194/gmdd-4-997-2011

Crockford RH, Richardson DP, 2000. Partitioning of rainfall into throughfall, stem-flow and interception: effect of forest type, ground cover and climate. Hydrol Process 14: 2903–2920. 3.0.CO;2-6" target="_blank">https://doi.org/10.1002/1099-1085(200011/12)14:16/17<2903::AID-HYP126>3.0.CO;2-6

Davies-Barnard T, Valdes PJ, Jones CD, Singarayer JS, 2014. Sensitivity of a coupled climate model to canopy interception capacity. Clim Dynam 42(7-8): 1715-1732. https://doi.org/10.1007/s00382-014-2100-1

Fischer G, Tubiello FN, van Velthuizen H, Wiberg DA, 2007. Climate change impacts on irrigation water requirements: Effects of mitigation, 1990–2080. Technol Forecast Soc 74: 1083–1107. https://doi.org/10.1016/j.techfore.2006.05.021

Ford ED, Deans JD, 1978. The effects of canopy structure on stemflow, throughfall and interception loss in a young sitka spruce plantation. J Appl Ecol 15(3): 905-917. https://doi.org/10.2307/2402786

FRWO (Forest, Range, and Watershed Organization of Iran), 2012. Project of Participatory Afforestation in the Zagros Region.

Friesen J, Lundquist J, Van Stan II JT, 2015. Evolution of forest precipitation water storage measurement methods. Hydrol Process 29: 2504–2520. https://doi.org/10.1002/hyp.10376

Goyal RK, 2004. Sensitivity of evapotranspiration to global warming: a case study of arid zone of Rajasthan (India). Agr Water Manage 69: 1–11. https://doi.org/10.1016/j.agwat.2004.03.014

Huntingford C, Zelazowski P, Galbraith D, Mercado LM, Sitch S, Fisher R, Lomas M, Walker A, Jones C, Booth, B, *et al.*, 2013. Simulated resilience of tropical rainforests to CO2-induced climate change. Nature Geoscience 6: 268–273. https://doi.org/10.1038/ngeo1741

Hempel S, Frieler K, Warszawski L, Schewe J, Piontek F, 2013. A trend-preserving bias correction - the ISI-MIP approach. Earth Syst Dynam 4(2): 219-236. https://doi.org/10.5194/esd-4-219-2013

Huntington TG, 2006. Evidence for intensification of the global water cycle: review and synthesis. J Hydrol 319: 83-95. https://doi.org/10.1016/j.jhydrol.2005.07.003

Hupet F, Vanclooster M, 2001. Effect of the sampling frequency of meteorological variables on the estimation of the reference evapotranspiration. J Hydrol 243: 192–204. https://doi.org/10.1016/S0022-1694(00)00413-3

Jazirei MH, 2009. Dryland Afforestation. University of Tehran Press, Iran. pp 560. ISBN 978-964-03-6122-1.

Jones CD, Hughes JK, Bellouin N, Hardiman SC, Jones GS, Knight J, Liddicoat S, O'Connor1 FM, Andres RJ, Bell C, *et al.*, 2011. The HadGEM2-ES implementation of CMIP5 centennial simulations. Geoscie Model Dev 4(3): 543-570. https://doi.org/10.5194/gmd-4-543-2011

Leng G, Tang Q, 2014. Modeling the impacts of future climate change on irrigation over China: sensitivity to adjusted projections. J Hydrometeorol 15(5): 2085-2103. https://doi.org/10.1175/JHM-D-13-0182.1

Levia DF, Frost EE, 2006. Variability of throughfall volume and solute inputs in wooded ecosystems. Prog Phys Geog 30: 605–632. https://doi.org/10.1177/0309133306071145

Levia DF, Keim RF, Carlyle-Moses DE, Frost EE, 2011. Throughfall and stemflow in wooded ecosystems, in Forest Hydrology and Biogeochemistry: Synthesis of Past Research and Future Directions, Ecol Studr Ser 216: 425–443.

Liu J, Song M, Horton RM, Hu Y, 2013. Reducing spread in climate model projections of a September ice-free arctic. P.12571-6 in Proc. of Conf. of National Academy of Sciences of the United States USA 110 (31).

McCuen RH, 1974. A sensitivity and error analysis of procedures used for estimating evaporation. Water Resour Bull 10 (3): 486–498. https://doi.org/10.1111/j.1752-1688.1974.tb00590.x

McGovern M, Pasher J, 2016. Canadian urban tree canopy cover and carbon sequestration status and change 1990–2012. Urban For Urban Gree 20: 227-232. https://doi.org/10.1016/j.ufug.2016.09.002

Miao C, Duan Q, Sun Q, Huang Y, Kong D, Yang T, Ye A, Di Zh, Gong W, 2014. Assessment of CMIP5 climate models and projected temperature changes over Northern Eurasia. Environ Res Lett. https://doi.org/10.1088/1748-9326/9/5/055007

Miralles DG, Gash JH, Holmes TRH, de Jeu RAM, Dolman AJ, 2010. Global canopy interception from satellite observations. J Geophys Res 115. https://doi.org/10.1029/2009JD013530

Moore LD, Van Stan II JT, Gay TE, Rosier C, Wu T, 2016. Alteration of soil chitinolytic bacterial and ammonia oxidizing archaeal community diversity by rainwater redistribution in an epiphyte-laden Quercus virginiana canopy. Soil Biol Biochem 100: 33-41. https://doi.org/10.1016/j.soilbio.2016.05.016

Moss RH, 2010. The next generation of scenarios for climate change research and assessment. Nat 463: 747–56. https://doi.org/10.1038/nature08823

Motahari M, Attarod P, Pypker TG, Etemad V, Shirvany A, 2013. Rainfall interception and canopy storage capacity of a Pinus eldarica plantation in a semi-arid climate zone: an application of the Gash model. J Agr Sci Tech-Iran 15: 981–994.

Muzylo A, Llorens P, Domingo F, 2012. Precipitation partitioning in a deciduous forest plot in leafed and leafless periods. Ecohydrology 5: 759–767. https://doi.org/10.1002/eco.266

Návar J, 2017. Fitting rainfall interception models to forest ecosystems of Mexico. J Hydrol 548: 458–470. https://doi.org/10.1016/j.jhydrol.2017.03.025

Pypker TG, Levia DF, Staelens J, Van Stan II JT, 2011. Canopy structure in relation to hydrological and biogeochemical fluxes. XVII. In: Levia, D.F., Carlyle-Moses, D.E., Tanaka, T. (Eds.), Forest Hydrology and Biogeochemistry: Synthesis of Past Research and Future Directions. Ecological Studies Series, Springer-Verlag, Heidelberg 216: 371–388. https://doi.org/10.1007/978-94-007-1363-5_18

Raat KJ, Draaijers GPJ, Schaap MG, Tietema A, Verstraten, JM, 2002. Spatial variability of throughfall water and chemistry and forest floor water content in a Douglas fir forest stand. Hydrol Earth Syst Sci 6: 363–374. https://doi.org/10.5194/hess-6-363-2002

Rosier CL, Van Stan II JT, Moore LD, Schrom JOS, Wu T, Reichard JS, Kan J, 2015. Forest canopy structural controls over throughfall affect soil microbial community structure in an epiphyte-laden maritime oak stand. Ecohydrology. https://doi.org/10.1002/eco.1595

Rutter AJ, Morton AJ, Robins PC, 1975. A predictive model of rainfall interception in forests II. Generalization of the model and comparison with observations in some coniferous and hardwood stands. J Appl Ecol 12: 367–380. https://doi.org/10.2307/2401739

Sadeghi SMM, Attarod P, Van Stan II JT, Pypker TG, Dunkerley D, 2015. Efficiency of the reformulated Gash's interception model in semiarid afforestations. Agr Forest Meteorol 201: 76-85. https://doi.org/10.1016/j.agrformet.2014.10.006

Sadeghi SMM, Attarod P, Van Stan II JT, Pypker TG, 2016. The importance of considering rainfall partitioning in afforestation initiatives in semiarid climates: A comparison of common planted tree species in Tehran, Iran. Sci Total Environ 568: 845-855. https://doi.org/10.1016/j.scitotenv.2016.06.048

Sagheb Talebi K, Sajedi T, Pourhashemi M, 2014. Forests of Iran, A treasure from the past, a hope for the future. Plant Vegetation 10: 149.

Shahid S, 2011. Impacts of climate change on irrigation water demand in northwestern Bangladesh. Climatic Change 105: 433–453. https://doi.org/10.1007/s10584-010-9895-5

Savenije HHG, 2004. The importance of interception and why we should delete the term evapotranspiration from our vocabulary. Hydrol Process 18(8): 1507-1511. https://doi.org/10.1002/hyp.5563

Singh VP, Xu C-Y, 1997. Sensitivity of mass transfer-based evaporation equations to errors in daily and monthly input data. Hydrol Process 11: 1465–1473. 3.0.CO;2-X" target="_blank">https://doi.org/10.1002/(SICI)1099-1085(199709)11:11<1465::AID-HYP452>3.0.CO;2-X

Staelens J, Schrijver AD, Verheyen K, Verhoest NEC, 2008. Precipitation partitioning into throughfall, stemflow, and interception within a single beech (Fagus sylvatica L.) canopy: influence of foliation, rain event characteristics,

and meteorology. Hydrol Process 2: 33-45. https://doi.org/10.1002/hyp.6610

Sun G, Zhou GY, Zhang ZQ, Wei XH, McNulty SG, Vose JM, 2006. Potential water yield reduction due to forestation across China. J Hydrol 328: 548–558. https://doi.org/10.1016/j.jhydrol.2005.12.013

Taylor KE, Stouffer RJ, Meehl GA, 2012. An overview of Cmip5 and the experiment design B. B Am Meteorol Soc 93: 485–98.

Toba T, Ohta T, 2005. An observational study of the factors that influence interception loss in boreal and temperate forests. J Hydrol 313: 208–220. https://doi.org/10.1016/j.jhydrol.2005.03.003

Tollefson J, 2016. Global warming already driving increases in precipitation extremes. Nature. https://doi.org/10.1038/nature.2016.19508

Ul Hassan M, Qureshi AS, Heydari N, 2007. A proposed framework for irrigation management transfer in Iran: Lessons from Asia and Iran. Colombo, Sri Lanka: International Water Management Institute. 37 pp. (IWMI Working Paper 118)

Valente F, David JS, Gash JHC, 1997. Modelling interception loss for two sparse eucalypt and pine forests in central Portugal using reformulated Rutter and Gash analytical models. J Hydrol 190: 141–162. https://doi.org/10.1016/S0022-1694(96)03066-1

Van Stan II JT, Godon DA, 2018. Mini-Review: Stemflow as a Resource Limitation to Near-Stem Soils. Front Plant Sci 9(248): 1-9. https://doi.org/10.3389/fpls.2018.00248

Vose S, Zimmermann B, Zimmermann A, 2016. Detecting spatial structures in throughfall data: The effect of extent, sample size, sampling design, and variogram estimation method. J Hydrol 540: 527-537. https://doi.org/10.1016/j.jhydrol.2016.06.042

Wallace J, Macfarlane C, McJannet D, Ellis T, Grigg A, Van Djik A, 2013. Evaluation of forest interception estimation in the continental scale Australian water resources assessment-landscape (AWRA-L) model. J Hydrol 499: 210–223. https://doi.org/10.1016/j.jhydrol.2013.06.036

Wang YH, Yu P, Feger KH, Wei X, Sun G, Bonell M, Xiong, W, Zhang S, Xu L, 2011. Annual runoff and evapotranspiration of forestlands and non-forestlands in selected basins of the Loess Plateau of China. Ecohydrology 4: 277–287. https://doi.org/10.1002/eco.215

Zhang Z, Zhao Y, Li X, Huang L, Tan H, 2016. Gross rainfall amount and maximum rainfall intensity in 60-minute influence on interception loss of shrubs: a 10-year observation in the Tengger Desert. Sci Rep-UK 6: 26030. https://doi.org/10.1038/srep26030